Chain Distortion of *m*-Linked Aromatic Polymers: Poly(*m*-phenylene) and Poly(*m*-pyridine)

Noritomo Kobayashi,*,† Shintaro Sasaki,† Masahiro Abe,‡ Shoutaro Watanabe,‡ Hiroki Fukumoto,‡ and Takakazu Yamamoto‡

Japan Advanced Institute of Science and Technology, 1-1 Asahidai, Tatsunokuchi, Nomi, Ishikawa 923-1292, Japan, and Chemical Resources Laboratory, Tokyo Institute of Technology, 4259 Nagatsuta, Midori-ku, Yokohama 226-8503, Japan

Received May 31, 2004; Revised Manuscript Received August 9, 2004

ABSTRACT: The crystal structures of poly(*m*-phenylene) (PMP) and poly(*m*-pyridine) [poly(pyridine-2,6-diyl)] (PMPy) have been analyzed by the linked-atom Rietveld method for X-ray powder diffraction profiles in order to demonstrate the effect of hydrogen repulsion on the planarity of aromatic polymer chains. Chain conformation of PMP is a slowly winding helix with a five-ring structural repeat, in which the neighboring aromatic rings are rotated owing to the hydrogen repulsion by torsion angles of average value 42°, in contrast to the alternately twisted conformation of poly(*p*-phenylene). The four helices are packed in a tetragonal unit cell with dimensions $a = b = 13.45$ Å and $c = 11.30$ Å (space group: $P4_12_12$ or $P4_32_12$), and they engage with one another. The helical structure, isomorphous to that of *m*-deciphenyl determined by single-crystal X-ray analysis, is stabilized by the interchain interactions. The PMPy chain assumes the anticoplanar conformation relieved from hydrogen repulsion. The two chains are contained in an orthorhombic unit cell with dimensions $a = 12.23$ Å, $b = 3.92$ Å, and $c = 7.06$ Å (space group: *Pnam*) in a manner similar to orthorhombic polyethylene.

Introduction

Preferred planar conformations of π-conjugated polymers are distorted by interatomic repulsions concerning pendant atoms as well as hydrogens. Single-crystal X-ray diffraction (XRD) analyses of polyphenyl oligomers[1−5] revealed that the rings are alternately rotated with torsion angles (ϕ) of about 20°, owing to the *ortho*-hydrogen repulsion. At $\phi = 0°$ (coplanar conformation), the distance between these hydrogens is shorter than 1.9 Å, while it is over 2.0 Å at $\phi = 20°$. The chain conformation of poly(*p*-phenylene) (PPP) is similarly twisted alternately about the collinear axis (Chart 1),[6−8] although the conjugation will persist by the effective propagation of the electronic interactions.[9]

Introduction of *m*-phenylene moieties into chain backbone has induced the interruption of the conjugation.[9−12] Steric distortion is possibly responsible for the broken conjugation. The homopolymer poly(*m*-phenylene) (PMP) was first synthesized by one of the present authors and shown to be crystalline.[13] Williams et al.[14] determined by single-crystal XRD analysis that an oligomer, *m*-deciphenyl, took a slowly winding helical conformation containing five rings in the turn and that the adjacent molecules engaged closely in a tetragonal unit cell with dimensions $a = b = 13.45$ Å and $c = 11.22$ Å. The space group was $P4_12_12$ or enantiomorphous $P4_32_12$, indicating that the crystals of the right-handed helices were separated from those of the left-handed ones. They also showed that intensities and positions of the reflection lines calculated for *m*-deciphenyl crystal were consistent with the profile of PMP. In the communication, however, the overall crystal structure was not described in detail. If the structures of *m*-deciphenyl and PMP are isomorphous, the chain conformation of

Chart 1

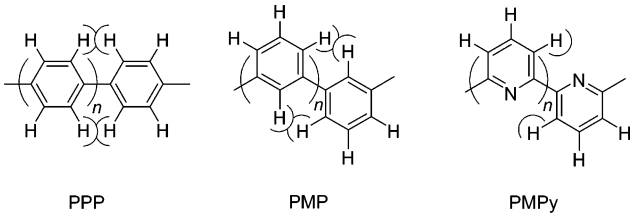

PMP is nearly the right-handed helix s(5/1)[15] for $P4_12_12$ or the left-handed one s(5/4) for $P4_32_12$. From the quantum-chemical study, Hong et al.[9] suggested that PMP chain could take two roughly isoenergetic helical conformations s(5/1) and s(5/2). The former coincides with the result of Williams et al.,[14] while the latter has not been observed yet. Furthermore, they demonstrated that the weak conjugation of *m*-phenylene sequences is not due to the steric distortion, but to the inherent nodal nature of the frontier molecular orbitals. As they pointed out for PPP, however, steric distortion has a great influence on the electronic structure.

Helical structures have been also suggested for PMP derivatives[16] and *m*-phenylene ethynylene oligomers[17] having chiral substituents, but the helical parameters are not clear.

On the other hand, poly(pyridine)s constituted of another fundamental aromatic ring have received less attention when compared with PPP. Poly(pyridine-2,5-diyl) and poly(2,2′-bipyridine-5,5′-diyl) (PBPy) showed a similar XRD pattern. The diffraction angles were quite different from those of the electron diffraction pattern of the vacuum-deposited PBPy single crystal.[18] In the latter case, the chains stand upright on the carbon substrate and are packed in *pgg* unit cell with dimensions $a = 8.06$ Å, $b = 5.75$ Å as in orthorhombic polyethylene (PE) and PPP.[6] In the as-polymerized powder sample, PBPy chains are stacked face to face in a *cmm* unit cell with $a = 10.8$ Å and $b = 3.76$ Å.[19]

† Japan Advanced Institute of Science and Technology.
‡ Tokyo Institute of Technology.
* Corresponding author. E-mail: n-kobaya@jaist.ac.jp.

10.1021/ma048923s CCC: $27.50
Published on Web 09/21/2004

The poly(*p*-pyridine) chains are possibly twisted alternately, owing to the *ortho*-hydrogen repulsion as in PPP, but the observed XRD profile was insufficient to detect the distortion.

On the basis of the result of Williams et al.,[14] we have performed the linked-atom Rietveld profile-fitting analysis (LARV) for PMP and also for poly(*m*-pyridine) [poly(pyridine-2,6-diyl)] (PMPy). In contrast to PMP, PMPy can assume the anticoplanar s(2/1) conformation relieved from the steric repulsion of hydrogens (Chart 1).

To cope with limited XRD data for polymers, the linked-atom least-squares method has been developed,[20−22] in which the number of refined parameters is reduced by constraining bond lengths and bond angles to their standard values. The crystal structure analysis of the α form of poly(L-lactide) has been successfully achieved by this technique.[23] The method, however, employs the integrated intensities of separate reflections and therefore cannot correspond to the low-resolution profile. In the meantime, the problem of overlapping of reflections has been addressed by the Rietveld whole-fitting method,[24,25] in which the loss of information can be recovered by the use of the composite profile. The combined Rietveld method, employing a linked-atom molecular model, has been successfully applied to structure determinations of PPP,[6] polythiophenes,[26−28] and other polymers.[29−36]

Experimental Section

Materials. PMP was prepared as previously reported.[37] The number-average degree of polymerization (DP) was estimated to be 45 by the polystyrene-standard GPC analysis for the nitrated polymer soluble in THF. PMPy was prepared by dehalogenative polycondensation[18] of 2,6-dibromopyridine using a zerovalent nickel complex. 2,6-Dibromopyridine (950 mg, 4.0 mmol) was added to a DMF (15 mL) solution containing bis(1,5-cyclooctadiene)nickel(0) (4.8 mmol), 1,5-cyclooctadiene (0.80 mL), and 2,2′-bipyridiyl (0.75 g, 4.8 mmol). After stirring for 4 days at 60 °C, the reaction mixture was poured into a mixture of methanol and diluted hydrobromic acid. The precipitate was washed repeatedly with aqueous solutions of tetrasodium salt of ethylenediaminetetraacetic acid, water, and methanol and dried under vacuum. Light scattering analysis in formic acid indicated that the polymer had a weight-average molecular weight of 3600, corresponding to DP of 47. Recently, preparation of poly(*m*-pyridine) by a different organometallic process was reported,[38] and the UV−vis curve of the present polymer agreed with that of poly(*m*-pyridine) shown in the paper.

The densities of the powder samples were measured at 25 °C by the flotation method using KBr aqueous solution or mixed solvents of methanol and carbon tetrachloride.

X-ray Diffraction. XRD profiles were measured with Cu Kα radiation (wavelength $\lambda = 1.5418$ Å) by using a Rigaku diffractometer equipped with a graphite monochromator and a scintillation counter. The data were accumulated over three time scans with a step of 0.1° in the range of diffraction angle $2\theta = 5-40°$.

In the present LARV analysis, reflection profiles were represented by Cauchy functions. The profile of the ith reflection was expressed by $f_i(2\theta) = (C_i/H_i)/(1 + 4z^2)$ with $z = (2\theta - 2\theta_0 - 2\theta_i)/H_i$, where C_i is proportional to the integrated intensity, H_i is the half-width, and $2\theta_0$ is the zero-angle correction. The dependence of H on θ has been formulated by a relation $H^2 = U \tan^2\theta + V \tan\theta + W$.[24,39] For analysis in the small 2θ range, the factor U is insignificant. It was replaced with a new term by taking into account the lattice disorder characteristic of aromatic polymers. As in PPP[6] and some poly(arylene)s,[18,27,28,40] the two-dimensional lateral packing of aromatic chains is generally ordered while the chain positions along the axes are rather disordered because of the chain rigidity and strong interchain interactions. The lth layer-line reflections are thus broadened with increasing layer-line coordinate $\zeta = l\lambda/c$. Accordingly, we have assumed the expression $H^2 = U\zeta + V \tan\theta + W$. The background scattering was approximated by a linear function of 2θ and a few broad Cauchy functions. The effect of preferred orientation introduced by Rietveld was neglected. Intensities were scaled by a factor k to absolute values expressed by $I/I_e v = \sum L_i |F_i|^2 f_i(2\theta)/v_c^2$, where I_e is the intensity scattered by a single electron, v is the scattering volume, L_i is the Lorentz polarization factor, F_i is the crystal structure factor, $f_i(2\theta)$ is the normalized profile function, and v_c is the unit cell volume. The structure factors were calculated by incorporating all the atoms as well as the hydrogen atoms with an overall isotropic temperature factor B. The factor B was fixed at some preset values, since the XRD data were insufficient to refine it as a parameter. The discrepancy between the observed (I_o) and calculated (I_c) intensities was evaluated by factors $R_p = \sum|I_o - I_c|/\sum I_o$ and $R_{wp} = \{\sum w|I_o - I_c|^2/\sum w I_o^2\}^{0.5}$, where the weight w was taken as reciprocal I_o.[41]

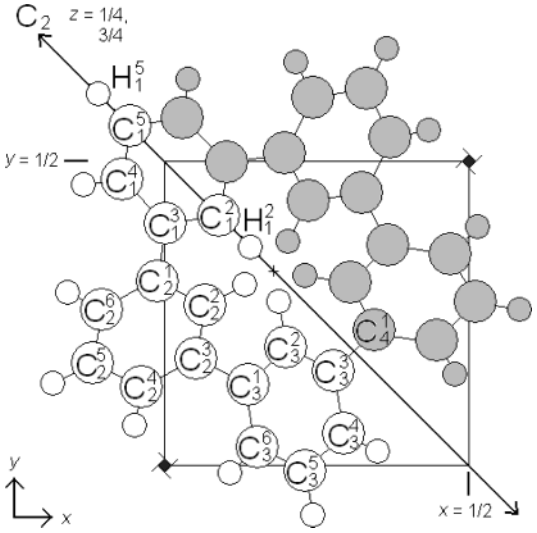

Figure 1. A uniform s(5/1) helix projected on a quarter of *ab* plane of the unit cell. The fractional coordinates of the shadowed atoms are generated by C_2 diad transformation ($-y + 0.5$, $-x + 0.5$, $-z + 0.5$).

Results and Discussion

Primary Structure of PMP. Packing models were constructed by arranging the uniform s(5/1) helices in the $P4_12_12$ unit cell with dimensions reported for *m*-deciphenyl. The corners of the unit cell were chosen at 4_1 axes. The molecular model was built with the bond lengths 1.50 Å for the inter-ring C−C bonds, 1.39 Å for the remaining C−C bonds, and 1.0 Å for the C−H bonds and all the bond angles 120°. To reproduce the *c* repeat distances 11.2−11.3 Å, the biaryl bond length was tentatively assumed to be 1.50 Å at this stage. According to the Miyazawa equation,[42] the uniform s(5/1) conformation of D_5 symmetry is realized by the inter-ring torsion angle $\phi = 41.81°$ and gives rise to the repeat distance $c = 11.25$ Å. The centers of the aromatic rings are apart by 3.1 Å from the helix axis.

Figure 1 draws a single chain viewed along the axis, where C_i^j designates the jth carbon atom in the ith aromatic ring and H_i^j the hydrogen atom attached to C_i^j. The crystallographic C_2 diad axes pass through the $H_1^5-C_1^5-C_1^2-H_1^2$ line, or the center of the $C_3^3-C_4^1$ bond, and the 2.5 aromatic rings comprise an asymmetric unit. The structural parameter is only the chain position along the C_2 axis. When the helix axis was at $(x, y) = (0.18, 0.32)$, the best fit between the observed

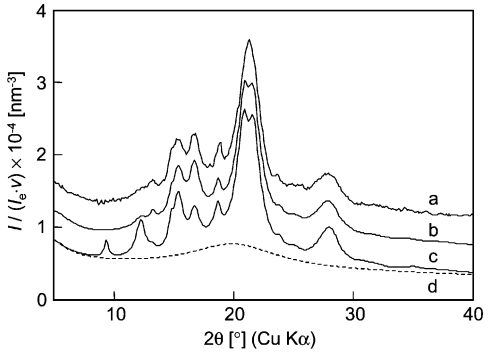

Figure 2. XRD profiles of PMP. Observed (a), calculated (b) for the distorted-helix model, and calculated (c) for the uniform-helix model. Curve a is shifted upward by 8000 and curve b by 4000 for visual obviousness. Curve d indicates assumed background scattering for curve c.

Table 1. X-ray Reflection Data of PMP

2θ/deg	d_{obs}/Å	d_{calc}/Å[a]	indices
13.2	6.7	6.73	200
14.8	6.0	6.02	210
15.3	5.79	5.78	201
16.7	5.31	5.31	211
18.9	4.7	4.76	220
21.3	4.2	4.33	202
		4.25	310
		4.12	212
28.0	~3.2	3.29	203
		3.22	401
		3.19	213
		3.13	411
		3.05	331

[a] Calculation is based on the tetragonal unit cell with $a = b =$ 13.45 Å and $c = 11.30$ Å.

and calculated profiles was obtained, but it involved serious discrepancies around $2\theta = 9.3°$ and 12.2° (curves a and c in Figure 2). It was expected that these discrepancies might be improved by the distortion from the uniform helix into the t2 helix.[15]

Crystal Structure Refinement of PMP. The helix was distorted by the six internal parameters: the bond lengths (r) and the torsion angles (ϕ) for three inter-ring bonds $C_1^3-C_2^1$ ($\equiv C_5^3-C_6^1$), $C_2^3-C_3^1$ ($\equiv C_4^3-C_5^1$), and $C_3^3-C_4^1$. Since there are four constraint conditions for the t2 chain to repeat with a distance c, the internal degree of freedom is only 2. The position of the C_1^2 atom as the origin along the C_2 axis is also a structural parameter. The nonstructural parameters are scale factor k, width parameters U, V, and W, zero-angle correction $2\theta_0$, and eight parameters to express the amorphous background (one straight line and two Cauchy functions). The quality of the present XRD data was not so fine to treat all the adjustable parameters in LARV least-squares refinements. To reduce the number of the variables, the refinements were repeated with various preset values of the temperature factor B, the background parameters, and also the unit cell dimensions. Some of the trials fell to false structures with abnormal bond lengths, but others yielded nearly the same structure. As is shown by curves a and b in Figure 2, the best fit between observed and calculated profiles ($R_p = 0.03$, $R_{wp} = 0.04$) was obtained for $B = 5$ Å^2, $2\theta_0 = 0.01°$, $c = 11.30$ Å, $U = 6.20$, $V = 0.15$, and $W = 0.25$ (for H in degrees). Table 1 lists d-spacing data of major reflections. The calculated density 1.24 g cm^{-3} is consistent with the observed value 1.20 g cm^{-3}. The refined values of the essential parameters (Table 2) are very close to those of Williams et al.[14] It has been pointed out that standard deviations derived from the diagonal terms of the inverse matrix of normal equation are generally underestimated in the Rietveld method and cannot be measures of accuracy. From the results of the LARV trials, they were estimated to be ca. 0.02 Å for bond lengths and ca. 1° for torsion angles. Atomic fractional coordinates are listed in Table 3. Standard deviations of orthogonal coordinates were estimated to be ca. 0.02 Å. Figure 3 illustrates the crystal structure of PMP, in which individual chains related by 4_1 axis at a corner are drawn in different colors. The helices engage with each other to fill the interspaces between them. In the projection onto the ab plane, the engagements form a kind of patchwork pattern.

Table 2. Internal Parameters of PMP

parameter	this work	Williams et al.[14]
$r(C_1^3-C_2^1)$	1.48 Å	1.47 Å
$r(C_2^3-C_3^1)$	1.50 Å	1.50 Å
$r(C_3^3-C_4^1)$	1.49 Å	1.49 Å
$\phi(C_1^3-C_2^1)$	46.0°	44°
$\phi(C_2^3-C_3^1)$	32.2°	34°
$\phi(C_3^3-C_4^1)$	54.3°	53°

Table 3. Atomic Fractional Coordinates of PMP[a]

atom	x	y	z
$C_1^{2\,b}$	0.096	0.404	−0.250
C_1^3	0.008	0.389	−0.188
C_1^4	−0.065	0.463	−0.188
$C_1^{5\,b}$	−0.050	0.550	−0.250
$H_1^{2\,b}$	0.148	0.352	−0.250
H_1^4	−0.128	0.452	−0.143
$H_1^{5\,b}$	−0.103	0.603	−0.250
C_2^1	−0.008	0.296	−0.121
C_2^2	0.067	0.258	−0.050
C_2^3	0.053	0.171	0.013
C_2^4	−0.037	0.120	0.004
C_2^5	−0.112	0.158	-0.068
C_2^6	−0.098	0.246	-0.131
H_2^2	0.132	0.295	-0.043
H_2^4	−0.048	0.057	0.048
H_2^5	−0.177	0.121	−0.075
H_2^6	−0.152	0.273	−0.182
C_3^1	0.134	0.130	0.090
C_3^2	0.198	0.195	0.148
C_3^3	0.274	0.157	0.219
C_3^4	0.284	0.055	0.234
C_3^5	0.219	−0.010	0.176
C_3^6	0.144	0.028	0.105
H_3^2	0.191	0.268	0.137
H_3^4	0.338	0.028	0.285
H_3^5	0.227	−0.083	0.187
H_3^6	0.098	−0.019	0.063

[a] The four chains are generated by the trans-formations; 1: (x, y, z), ($-y + 0.5$, $-x + 0.5$, $-z + 0.5$); 2: ($-y$, x, $z + 0.25$), ($x - 0.5$, $-y + 0.5$, $-z + 0.75$); 3: ($-x$, $-y$, $z + 0.5$), ($y - 0.5$, $x - 0.5$, $-z$); 4: (y, $-x$, $z + 0.75$), ($-x + 0.5$, $y - 0.5$, $-z + 0.25$). [b] The four atoms are placed on special positions (C_2 diad axis in Figure 1) with a half-occupancy.

Interchain Interactions in PMP. There is no seriously abnormal interatomic contact in PMP crystal. The crystal density 1.24 g cm^{-3} is lower than that of PPP (1.39 g cm^{-3}). The ring planes are tilted by angles of average value 37° from the horizontal plane normal to the chain axis. The interpenetrated rings of neighboring chains are not parallel. Therefore, the engagements differ from face-to-face stacking. In this sense, it is considered that the chains are weakly interacted with one another.

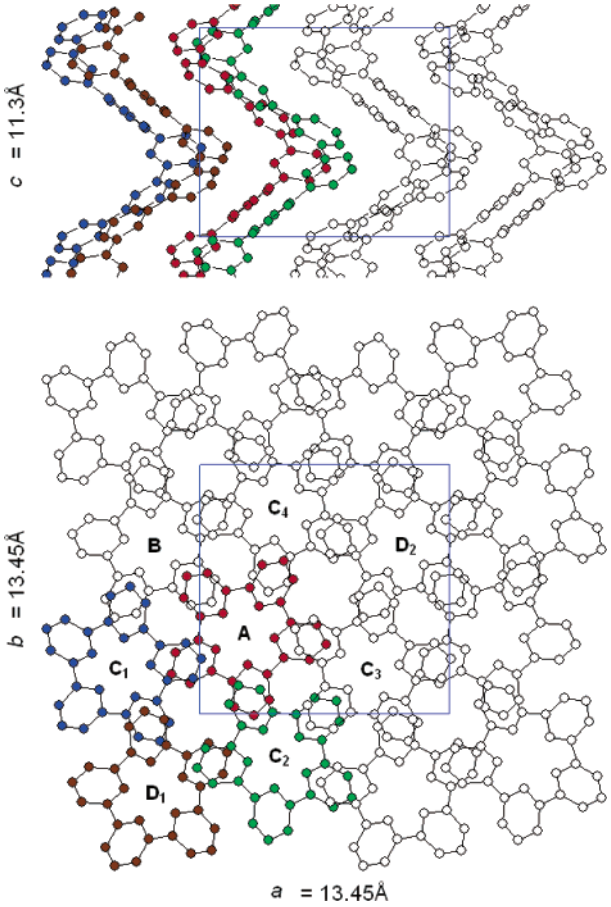

Figure 3. Crystal structure of PMP: upper, *ac* projection; lower, *ab* projection.

Individual chains engage with five chains. For instance, chain A in Figure 3 is surrounded by chains B, C_1, C_2, C_3, and C_4. Chain A is interrelated with B by the crystallographic 2_1 axis along the *c* axis and with C chains by the 4_1 axis. Furthermore, chain A does not engage directly with, but faces to, chains D_1 and D_2. Accordingly, there are three kinds of interchain interactions, namely, one 2_1 interaction (E_1), four 4_1 interactions (E_2), and two 4_1^2 interactions (E_3).

Interchain interaction energies were evaluated per monomeric unit by using Lennard-Jones 6−12 potential functions with van der Waals minimum $R^* = 1.85$ Å and well depth $\epsilon^* = 0.12$ kcal/mol for carbon atom and $R^* = 1.10$ Å and $\epsilon^* = 0.03$ kcal/mol for the hydrogen atom.[43] The uniform-helix model and the refined distorted-helix model were roughly isoenergetic; $E_1 \sim E_2 \sim -3$ kcal/mol and $E_3 \sim -0.7$ kcal/mol. The packing energy as half the sum of the interaction energies was ca. −8 kcal/mol. In the uniform-helix model, several short interchain C···C distances of ca. 3.4 Å were observed in the E_2 interaction, while these were removed by the helix distortion.

In contrast to s(5/1), the s(5/2) helix proposed by Hong et al.[9] is slim, and the neighboring chains cannot interpenetrate with one another. The inter-ring torsion angle is 138.19°, and the repeat distance is 18.20 Å. The centers of the aromatic rings are apart by 1.18 Å from the helix axis, and the ring planes are nearly parallel to the chain axis. The van der Waals interchain interaction energy minimized for a couple of parallel chains was ca. −1.7 kcal/mol when the lateral and axial displacements were 5.75 and 1.82 Å, respectively. The density is to be 1.21 g cm^{-3} for pseudohexagonal packing of $a = 5.75$ Å, although the 5-fold screw symmetry cannot be suited to any crystallographic symmetry. The packing energy is −5 kcal/mol at most. The s(5/2) structure is clearly unfavorable in the interchain interactions.

Table 4. X-ray Reflection Data of PMPy

2θ/deg	d_{obs}/Å	d_{calc}/Å[a]	indices
14.5	6.11	6.12	200
19.3	4.59	4.61	201
23.8	3.74	3.73	110
26.0	3.43	3.43	011
27.0	3.30	3.30	210
31.7	2.82	2.83	310
		2.81	401

[a] Calculation is based on the orthorhombic unit cell with $a = 12.23$ Å, $b = 3.92$ Å, and $c = 7.06$ Å.

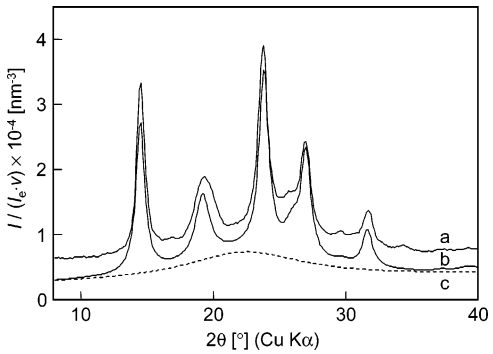

Figure 4. Comparison between observed (a) and calculated (b) profiles of PMPy. Curve a is shifted upward by 3000. Curve c indicates assumed background scattering for curve b.

Crystal Structure of PMPy. Sharp reflections were indexed as the equatorial ones of a rectangular unit cell with dimensions $a = 12.23$ Å and $b = 3.92$ Å (Table 4). The size of the unit cell and the high observed density (1.51 g cm^{-3}) supported the anticoplanar conformation with the repeated distance $c = 7.06$ Å. The calculated density agreed with the observed value. The molecular model of D_{2h} symmetry was constructed with bonds lengths of inter-ring C−C = 1.48 Å, intra-ring C−C = 1.38 Å, C−N = 1.34 Å, C−H = 1.00 Å, and backbone bond angles 116° and intra-ring bond angles 116°, 124°, 119°, 118°, 119°, and 124° by referring to the standard values.[41] The hydrogen atoms were attached outside on the line bisecting the bond angles. By taking into account atomic van der Waals radii and the closest chain packing, several packing models were constructed, and the diffraction curves were simulated. The space group turned out to be orthorhombic *Pnam* as in PE. The structural parameter was only the setting angle of the molecular plane against the *ac* plane, and it was refined to 27 ± 1°. The best fit between observed and calculated profiles ($R_p = 0.06$, $R_{wp} = 0.07$) was obtained with $B = 7$ Å^2, $U = 4.3$, $V = 1.1$, and $W = 0.5$ (Figure 4). The chain packing is shown in Figure 5.

It is certain that the PMPy chain is essentially planar. A question arises whether it is rigidly planar or distorted slightly. Actually, the N···H contact of ca. 2.4 Å is rather close if we do not allow for the hydrogen-bond character. Since the rotational C−C bonds are not collinear, the chain cannot adopt an alternately twisted structure. If the chain is distorted from the anticoplanar conformation, it will result in disorder. The widths of equatorial reflections, $H = (V \tan \theta + W)^{0.5} \sim 0.8°$ or

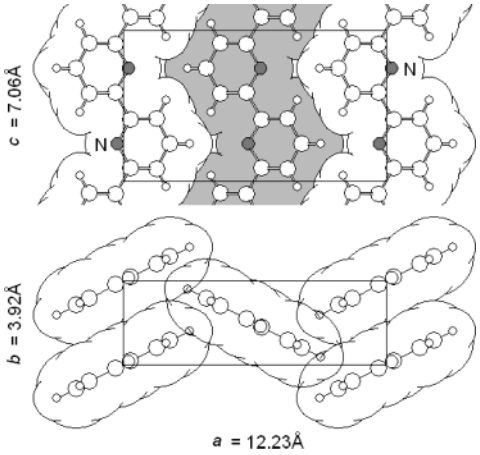

Figure 5. Crystal structure of PMPy: upper, *ac* projection; lower, *ab* projection. Atoms are illustrated with respective van der Waals radii.

$\Delta(2 \sin \theta/\lambda) = H \cos \theta/\lambda \sim 0.01$ Å^{-1} in the reciprocal space, are rather sharp and not so broadened with increasing 2θ. This indicates that the packing is well ordered. Widths of reflections from the crystal with size L and strain $\eta = \delta d/\langle d \rangle$ are approximated by an equation H (radian) $= \lambda/L \cos \theta + 2\eta \tan \theta$.[44] In comparison with the expression $H^2 = V \tan \theta + W$ for the equatorial reflections, we obtain $L \sim \lambda/W^{0.5}$ and $\eta \sim V/4W^{0.5}$. These lead to the mean lateral size $L \sim 120$ Å and the lattice strain $\eta \sim 0.006$. As inferred from the fairly small packing disorder, the chain distortion is not appreciable in PMPy.

Conclusions

It is thought that steric hydrogen repulsion is originally responsible for the s(5/1) conformation of PMP. The intrachain effect stabilizes the slowly winding unique helix cooperatively with the interchain interactions. In contrast to this, the s(5/2) model is nearly isoenergetic as an isolated single chain, but it is destabilized by the interchain interactions.

The PMP chain can be regarded as a sort of *cis*-linked polymer. In the rotational isomeric point of view, it resembles *cis*-polyacetylenes. Monosubstituted polyacetylenes take the helical conformation containing ca. 2.7 residues in the turn and aggregate in the columnar structure.[45] The s(8/3) or s(11/4) helix is close to s(5/2) rather than s(5/1). Unlike PMP, the helix core wears flexible substituents, and the interchain interactions are smeared in the liquid-crystalline structure.

In polymers having large pendant groups, the structure must accommodate the protrusions for the effective chain packing. Interchain interactions may play the leading role for the chain distortion. For instance, methyl-substituted PBPy assumes neither *pgg* nor *cmm* structure characteristic of the planar structure.[18] The analyses will be reported elsewhere.

Acknowledgment. We are grateful to Professor K. Kubota of Gunma University for determination of the molecular weight of PMPy by the light scattering analysis.

References and Notes

(1) Rietveld, H. M.; Maslen, E. N.; Clews, C. J. B. *Acta Crystallogr.* **1970**, *B26*, 693.
(2) Delugeard, Y.; Desuche, J.; Baudour, J.-L. *Acta Crystallogr.* **1976**, *B32*, 702.
(3) Baudour, J.-L.; Delugeard, Y.; Rivet, P. *Acta Crystallogr.* **1978**, *B34*, 625.
(4) Cailleau, H.; Baudour, J.-L.; Meinnel, J.; Dworkin, A.; Moussa, F.; Zeyen, C. M. E. *Faraday Discuss.* **1980**, *69*, 7.
(5) Baker, K. N.; Fratini, A. V.; Resch, T.; Knachel, H. C.; Adams, W. W.; Socci, E. P.; Farmer, B. L. *Polymer* **1993**, *34*, 1571.
(6) Sasaki, S.; Yamamoto, T.; Kanbara, T.; Morita, A.; Yamamoto, T. *J. Polym. Sci., Part B: Polym. Phys.* **1992**, *30*, 293.
(7) Ambrosch-Draxl, C.; Majewski, J. A.; Vogl, P.; Leising, G. *Phys. Rev. B* **1995**, *51*, 9668.
(8) Cuff, L.; Kertesz, M. *Macromolecules* **1994**, *27*, 762.
(9) Hong, S. Y.; Kim, D. Y.; Kim, C. Y.; Hoffmann, R. *Macromolecules* **2001**, *34*, 6474.
(10) Musfeldt, J. L.; Reynolds, J. R.; Tanner, D. B.; Ruiz, J. P.; Wang, J.; Pomerzntz, M. *J. Polym. Sci., Part B: Polym. Phys.* **1994**, *32*, 2395.
(11) Kang, B. S.; Kim, D. H.; Lim, S. M.; Kim, J.; Seo, M.-L.; Bark, K.-M.; Shin, S. C. *Macromolecules* **1997**, *30*, 7196.
(12) Pang, Y.; Li, J.; Hu, B.; Karasz, F. E. *Macromolecules* **1998**, *31*, 6730.
(13) Yamamoto, T.; Hayashi, Y.; Yamamoto, A. *Bull. Chem. Soc. Jpn.* **1978**, *51*, 2091.
(14) Williams, D. J.; Colquhoun, H. M.; O'Mahoney, C. A. *J. Chem. Soc., Chem. Commun.* **1994**, 1643.
(15) Allegra, G.; Corradini, P.; Elias, H.-G.; Geil, P. H.; Keith, H. D.; Wunderlich, B. *Pure Appl. Chem., Suppl.* **1989**, *61*, 769. In the IUPAC notation s(*A***M*/*N*), the helix class *A* identifies the number of skeletal atoms contained in the helix residue, and the integer *M* denotes the number of residues contained in *N* helical turns. The index *A* can be dropped if deemed unnecessary. The notation t2 means the symmetry elements of the translation along the chain axis and the 2-fold axis orthogonal to the chain axis.
(16) Suda, K.; Akagi, K. *Polym. Prepr. Jpn.* **2004**, *53*, 688.
(17) Goto, H.; Heemstra, J. M.; Hill, D. J.; Moore, J. S. *Org. Lett.* **2004**, *6*, 889.
(18) (a) Yamamoto, T.; Maruyama, T.; Zhou, Z.; Ito, T.; Fukuda, T.; Yoneda, Y.; Begum, F.; Ikeda, T.; Sasaki, S.; Takezoe, H.; Fukuda, A.; Kubota, K. *J. Am. Chem. Soc.* **1994**, *116*, 4832. (b) Yamamoto, T.; Kanbara, T.; Mori, C.; Wakayama, H.; Fukuda, T.; Inoue, T.; Sasaki, S. *J. Phys. Chem.* **1996**, *100*, 12631.
(19) Sasaki, S.; Yamamoto, T. *JAIST-POSTECH Joint Symp. Macromol. Sci.* **2002**, *2*, 37.
(20) (a) Arnott, S.; Wonacott, A. J. *Polymer* **1966**, *7*, 157. (b) Arnott, S.; Wonacott, A. J. *J. Mol. Biol.* **1966**, *21*, 371. (c) Arnott, S.; Selsing, E. *J. Mol. Biol.* **1974**, *88*, 509.
(21) (a) Takahashi, Y.; Tadokoro, H. *Macromolecules* **1973**, *6*, 672. (b) Takahashi, Y. *Macromolecules* **2003**, *36*, 8652. (c) Takahashi, Y.; Nishikawa, S. *Macromolecules* **2003**, *36*, 8656.
(22) (a) Sasaki, S.; Takahashi, Y.; Tadokoro, H. *J. Polym. Sci., Polym. Phys. Ed.* **1972**, *10*, 2362. (b) Sasaki, S.; Iwanami, Y. *Macromolecules* **1988**, *21*, 3389.
(23) Sasaki, S.; Asakura, T. *Macromolecules* **2003**, *36*, 8385.
(24) Rietveld, H. M. *J. Appl. Crystallogr.* **1969**, *2*, 65.
(25) *The Rietveld Method*; Young, R. A., Ed.; Oxford University Press: Oxford, 1993.
(26) Brückner, S.; Porzio, W. *Makromol. Chem.* **1988**, *189*, 961.
(27) Yamamoto, T.; Lee, B.-L.; Suganuma, H.; Sasaki, S. *Polym. J.* **1998**, *30*, 853.
(28) Sasaki, S.; Maehara, K.; Nurulla, I.; Yamamoto, T. *Polym. J.* **2000**, *32*, 984.
(29) (a) Brückner, S.; Di Silvestro, G.; Porzio, W. *Macromolecules* **1986**, *19*, 235. (b) Brückner, S.; Luzzati, S.; Porzio, W.; Sozzani, P. *Macromolecules* **1987**, *20*, 585.
(30) (a) Brückner, S.; Meille, S. V.; Porzio, W. *Polymer* **1988**, *29*, 1586. (b) Meille, S. V.; Brückner, S.; Lando, J. B. *Polymer* **1989**, *30*, 786.
(31) Ferro, D. R.; Brückner, S. *Macromolecules* **1989**, *22*, 2359.
(32) Meille, S. V.; Poletti, A. R.; Gallazzi, M. C.; Gleria, M.; Brückner, S. *Polymer* **1992**, *33*, 2364.
(33) Brückner, S.; De Rosa, C.; Corradini, P.; Porzio, W.; Musco, A. *Macromolecules* **1996**, *29*, 1535.
(34) Corradi, E.; Farina, A.; Gallazzi, M. C.; Brückner, S.; Meille, S. V. *Polymer* **1999**, *40*, 4473.
(35) (a) Iannelli, P. *Macromolecules* **1993**, *26*, 2303. (b) Acierno, D.; Concilio, S.; Maio, L. D.; Iannelli, P.; Lotz, B.; Scarfato, P. *Macromolecules* **2002**, *35*, 2288.
(36) (a) Colquhoun, H. M.; Dudman, C. C.; Blundell, D. J.; Bunn, A.; Williams, D. J. *Macromolecules* **1993**, *26*, 107. (b) Colqu-

houn, H. M.; Aldred, P. L.; Zhu, Z.; Williams, D. J. *Macromolecules* **2003**, *36*, 6416.
(37) Yamamoto, T.; Abe, M.; Takahashi, Y.; Kawata, K.; Kubota, K. *Polym. J.* **2003**, *35*, 603.
(38) Tammer, M.; Horsburg, L.; Monkman, A. P.; Brown, W.; Burrows, H. D. *Adv. Funct. Mater.* **2002**, *12*, 447.
(39) Caglioti, G.; Paoletti, A.; Ricci, F. P. *Nucl. Instrum.* **1958**, *3*, 223.
(40) (a) Yamamoto, T.; Ushiro, A.; Yamaguchi, I.; Sasaki, S. *Macromolecules* **2003**, *36*, 7075. (b) Yamamoto, T.; Muramatsu, Y.; Lee, B.-L.; Kokubo, H.; Sasaki, S.; Hasegawa, M.; Yagi, T.; Kubota, K. *Chem. Mater.* **2003**, *15*, 4384.
(41) *International Tables for Crystallography*; Wilson, A. J. C., Prince, E., Eds.; Kluwer: Dordrecht, 1999; Vol. C.
(42) Miyazawa, T. *J. Polym. Sci.* **1961**, *55*, 215.
(43) (a) Weiner, S. J.; Kollman, P. A.; Case, D. A.; Singh, U. C.; Ghio, C.; Alagona, G.; Profeta, S., Jr.; Weiner, P. *J. Am. Chem. Soc.* **1984**, *106*, 765. (b) Weiner, S. J.; Kollman, P. A.; Nguyen, D. T.; Case, D. A. *J. Comput. Chem.* **1986**, *7*, 230.
(44) (a) Hall, W. H. *Proc. Phys. Soc. London A* **1949**, *62*, 741. (b) Katayama, K. *J. Phys. Soc. Jpn.* **1961**, *16*, 462.
(45) (a) Tabata, M.; Sone, T.; Mawatari, Y.; Yonemoto, D.; Miyasaka, A.; Fukushima, T.; Sadahiro, Y. *Macromol. Symp.* **2003**, *192*, 75. (b) Kozuka, M.; Sone, T.; Sadahiro, Y.; Tabata, M.; Enoto, T. *Macromol. Chem. Phys.* **2002**, *203*, 66.

MA048923S